Multiwavelength Analysis of Quasi-Periodic Pulsations (QPPs) in a Solar Flare
PROGRESS REPORT no. 1

For the first progress report (and for the sake of learning), we reproduced the results from Clarke et al. (2021). Analysis was done through multiple steps, and here we're showing key plots and conclusions.

Image below illustrates Neupert effect. Basically, we have soft X-ray (SXR) and hard X-ray (HXR) light curves. SXR is obtained from Geostationary Operational Environmental Satellite (GOES) and HXR is obtained from Gamma-ray Space Telescope (GBM) onboard Fermi. We show time derivative of GOES light curve ($1-8$Å channel) and Fermi GBM ($25-50$ keV) light curve, on the same plot. This way, HXR flux from the flare *footpoints* is related to the thermal SXRs observed from plasma.

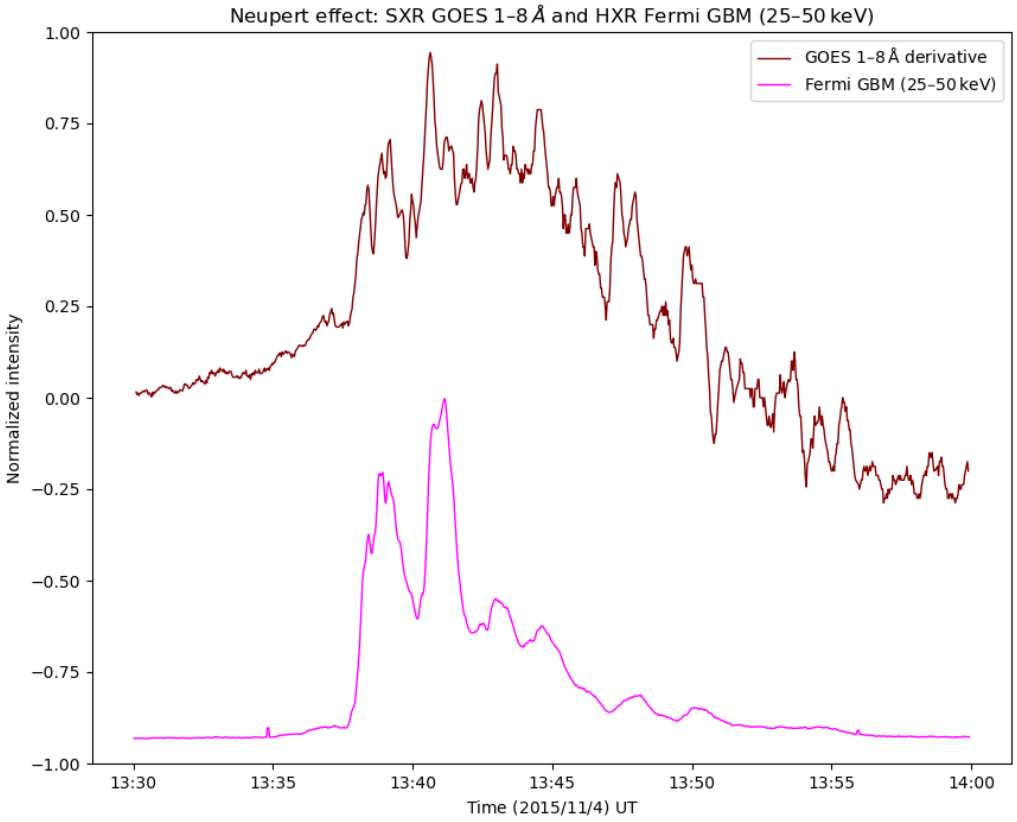

We continue by showing next plot, that is sort of a summary (we plot all relevant light curves we work with, along dynamic spectrum [radio wavelength], because we can use these data to determine information about the periodicity and location of the QPPs).

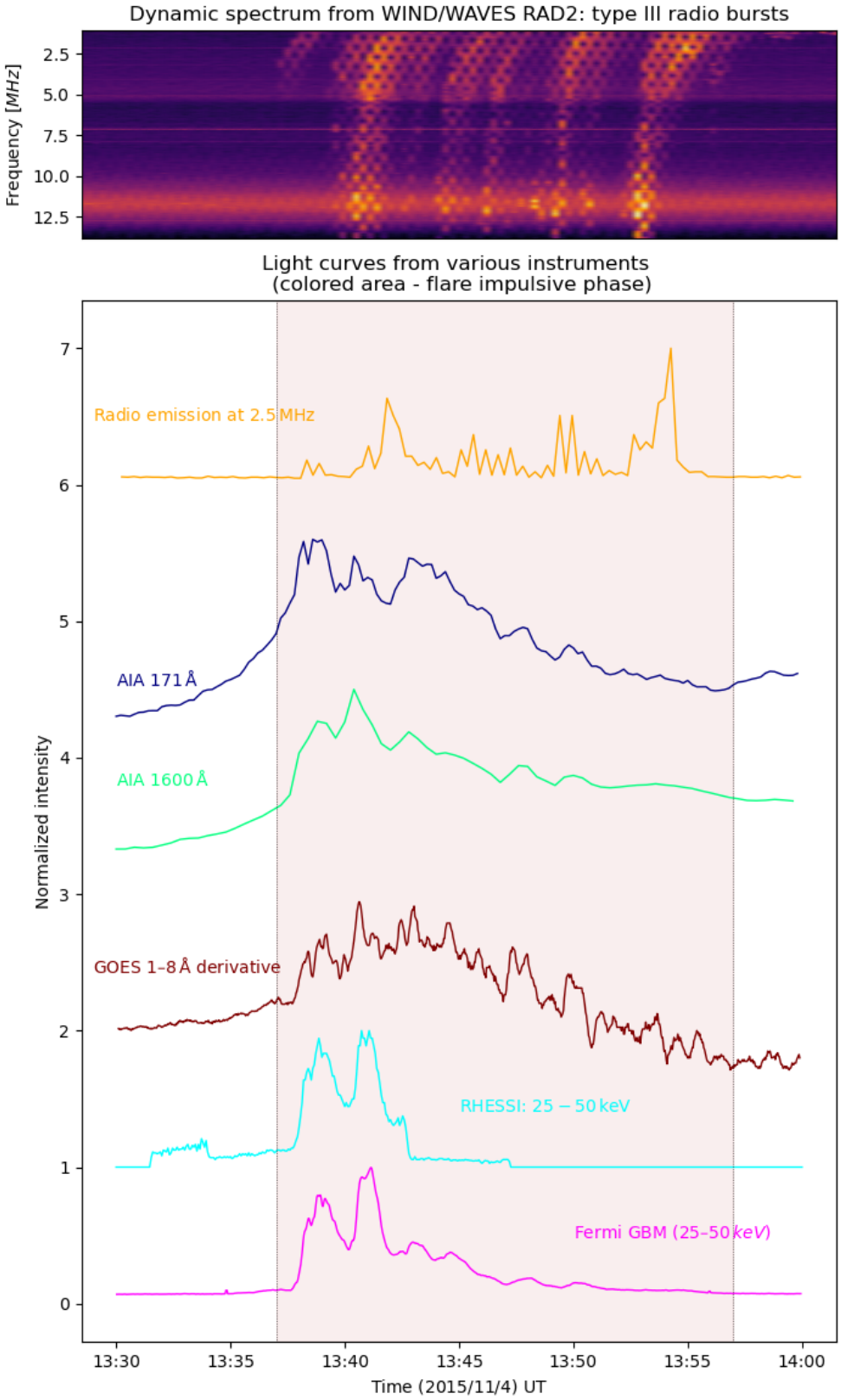
Dynamic spectrum from WIND/WAVES RAD2: type III radio bursts
Frequency [MHz]
2.5
5.0
7.5
10.0
12.5
Light curves from various instruments
(colored area - flare impulsive phase)
Radio emission at 2.5 MHz
AIA 171 Å
AIA 1600 Å
GOES 1–8 Å derivative
RHESSI: 25 – 50 keV
Fermi GBM (25–50 keV)
Normalized intensity
0
1
2
3
4
5
6
7
13:30
13:35
13:40
13:45
13:50
13:55
14:00
Time (2015/11/4) UT

Furthermore, we show wavelet analysis results. Morlet wavelet algorithm was applied to the multi-wavelength light curves to determine their periodicities. We show only one example, where analysis was conducted on detrended HXR emission from the flare (similar results were obtained when detrending wasn't included). Table with the results from wavelet[1] is also given.

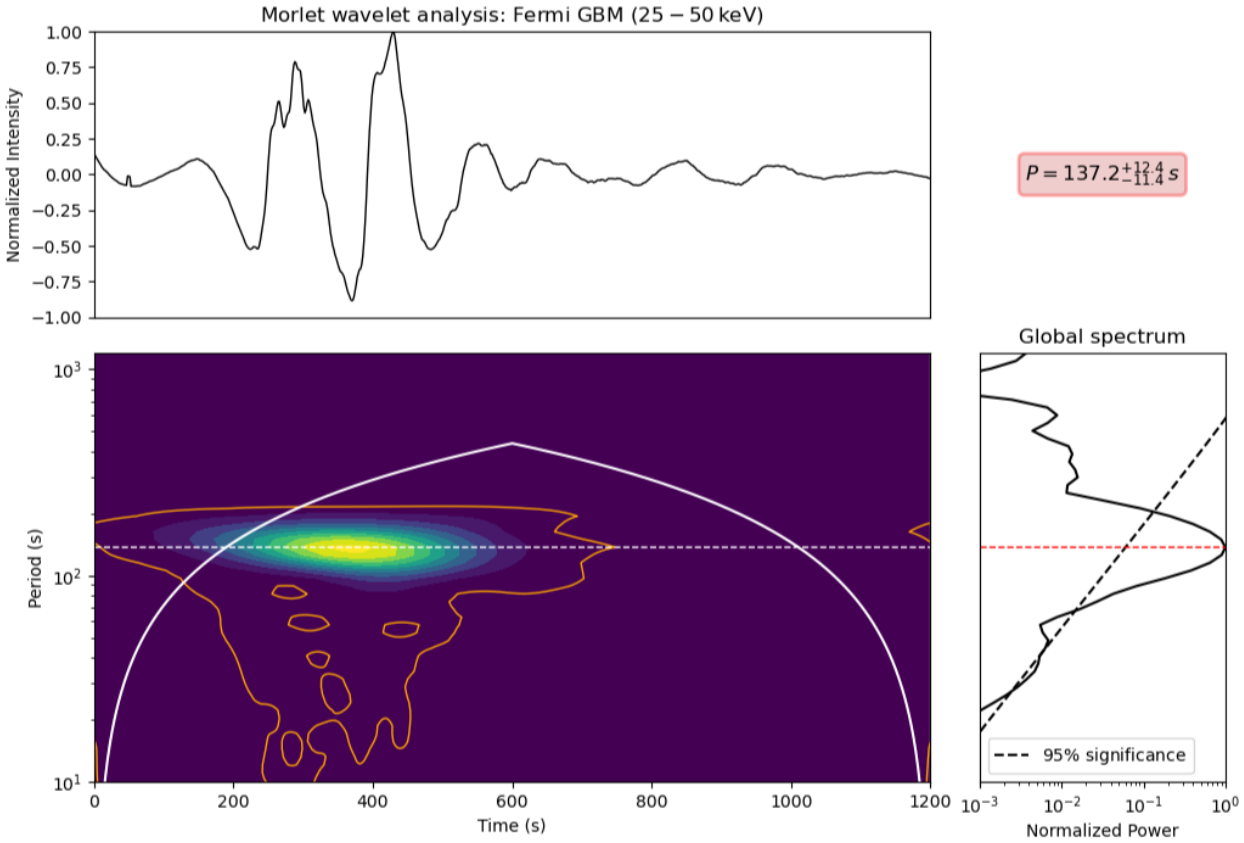

λ	2.5 MHz	171 Å	1600 Å	1–8 Å	25–50 keV
Period (s)	225^{+20}_{-19}	129^{+12}_{-11}	140^{+13}_{-12}	121^{+11}_{-10}	137^{+12}_{-11}
Δt (s)	16.2	12.0	24.0	2.0	1.6

Wavelet analysis - period estimation for different light curves.

In addition to this, we estimated periods manually, by visually identifying peaks. We'll use GOES derivative plot as an example for peak identification. After that, plot *time vs. pulsation number* is displayed, to demonstrate core of this alternative period finding method - slope on the line on that plot provides an estimate of period.

[1]Detrending is included in wavelet analysis, for every light curve.

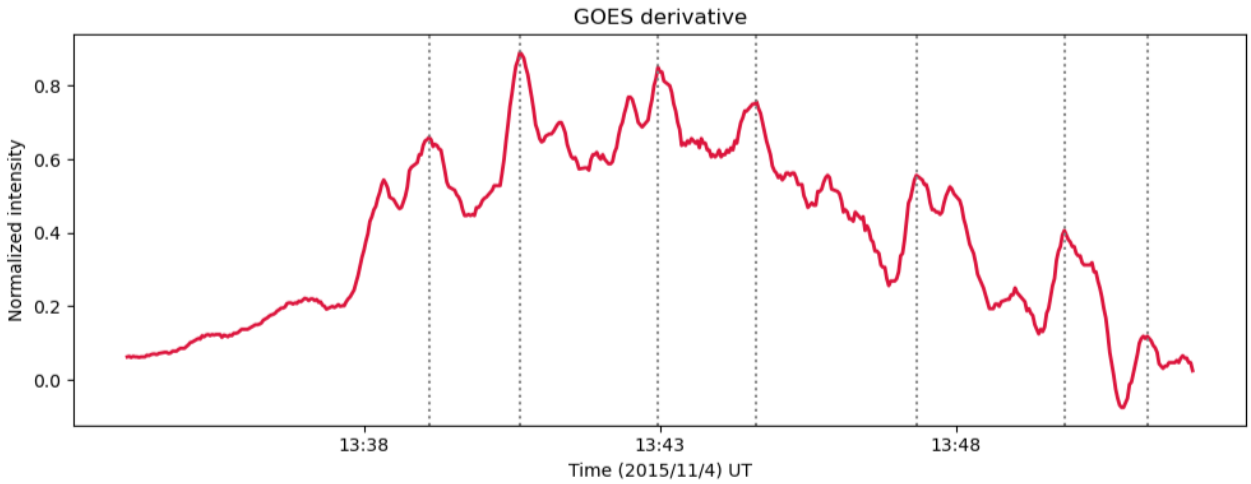

The peaks identified show approximate temporal agreement, which holds for all higher-frequency data considered. That was needed, in order to perform further analysis.

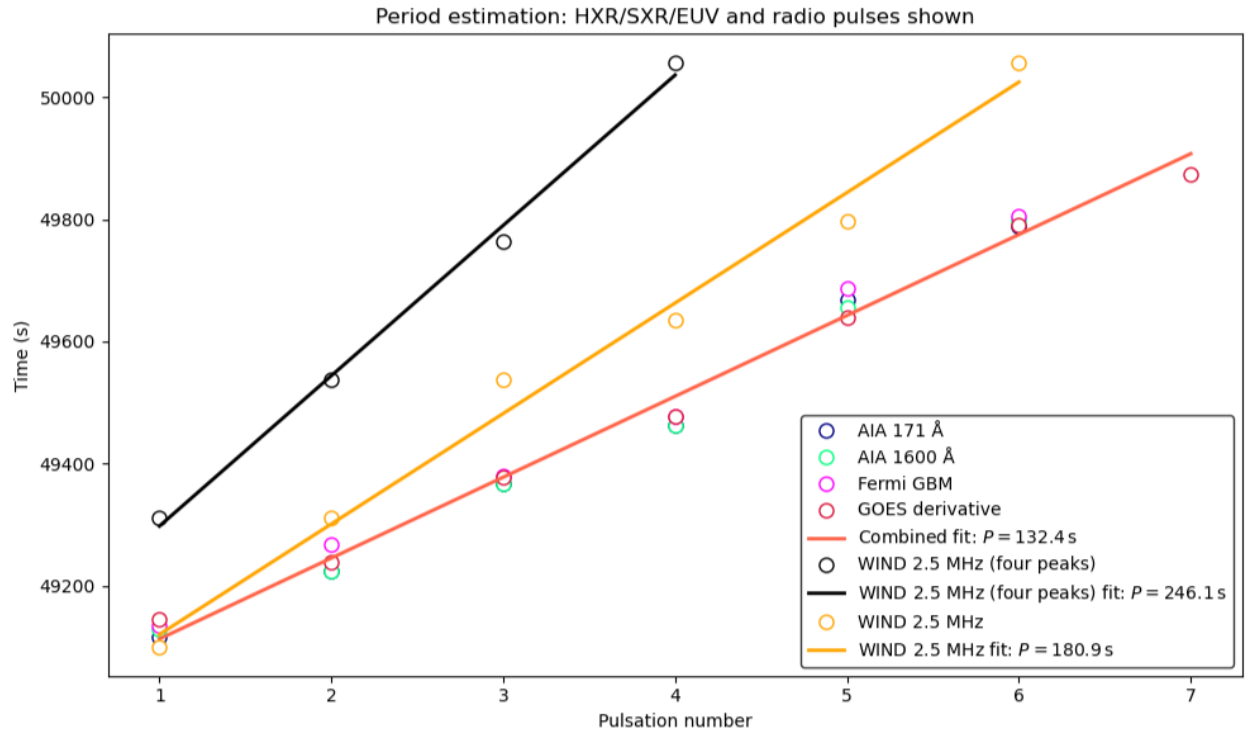

Six (seven) HXR/SXR/EUV[2] pulses shown above are plotted using the circle symbols. Straight line is fitted to these, and we obtained period of $\sim 134\,\mathrm{s}$ (good agreement with wavelet results). For the radio emission at 2.5 MHz, this analysis was done for the four main peaks in the time series. We also included more peaks of lower amplitude and plotted that case too. Lower period is obtained when more peaks are included.

[2]Extreme Ultraviolet.

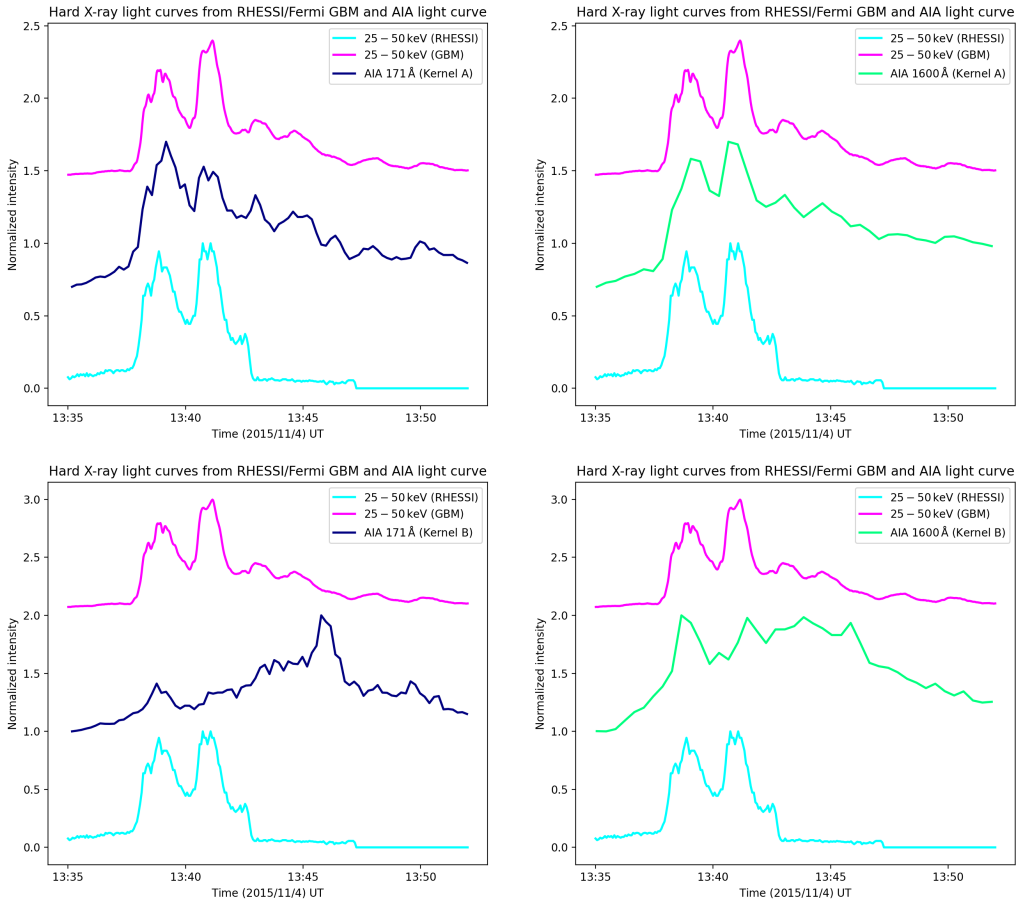

Since we couldn't use PIXON[3] algorithm to determine where the non-thermal HXRs originated from, we performed modified spatial analysis of QPPs. We denoted one kernel (A) in the flaring region and the other one (B) a little bit outside (both relatively small). We extracted AIA light curves (both in 171 Å and 1600 Å) and compared those to the RHESSI and GBM HXR light curves. It was found that kernel A AIA light curves correlate to the HXR light curves more than kernel B AIA light curves. This approximately localizes the source of QPPs close to that region.

To solidify these findings[4], we performed potential field source surface (PFSS) extrapolation, and identified open magnetic field lines. PFSS model provides an approximation of the coronal magnetic field up to $2.5\,R_\odot$, based on the observed photospheric field. The goal is to connect kernel A with open field source, in order to explain bursty magnetic reconnection via interaction between closed and open field lines. Plot that shows this can be greatly improved, and is given on the next page.

[3]PIXON relies on IDL, which we do not have access to. Instead, we tried to implement a nearest-neighbor dirty-map reconstruction to generate the RHESSI HXR images. That wasn't really successful!

[4]We also estimated the height of the source producing radio emission. The height is $\sim 16.2 R_\odot$. We used Newkirk electron density model (1967).

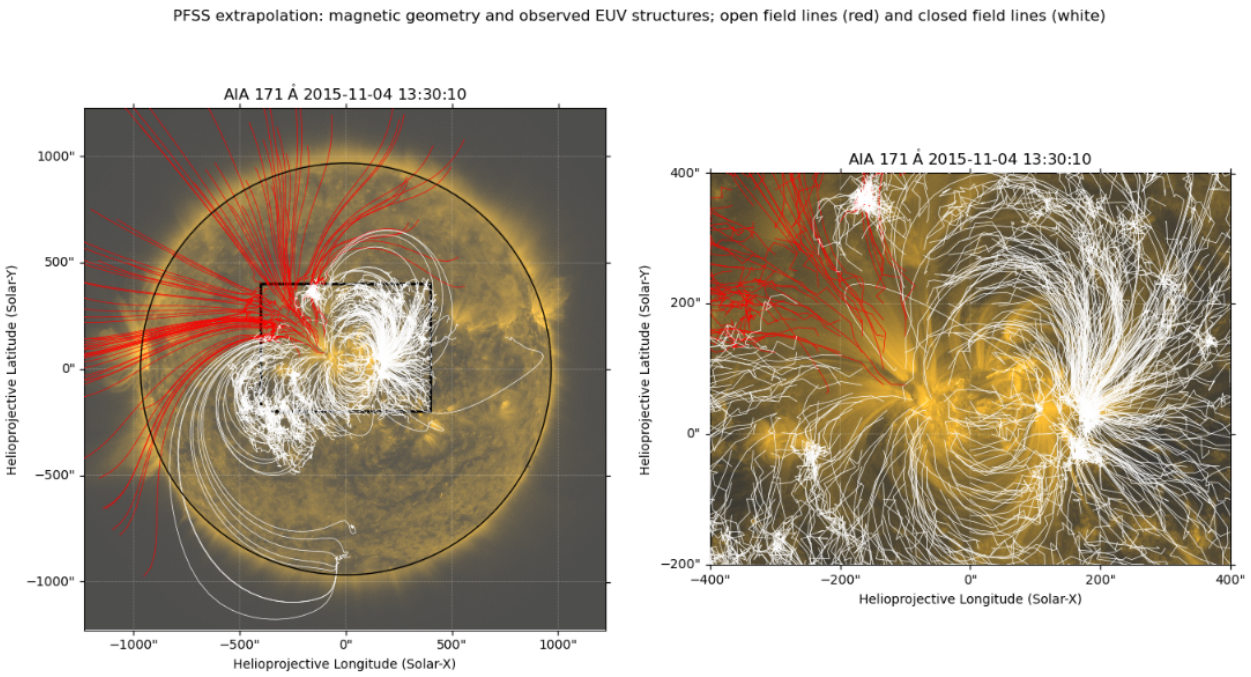

Additional remarks

1. In the paper, cubic-spline fit is used to remove the slow background before doing wavelets. We used Savitzky–Golay (SG) filter, since we've found it superior. It adapts locally, with no need to pick knots, and tends to preserve peak amplitudes and widths far better than a *global* spline. Also, it has sharper edge-preservation and it's easier to tune. We think it's somehow more robust when there's jitter in the data, but this needs to be checked.

2. An actual calculation of the correlation between AIA light curves extracted from kernels and HXR light curves would be helpful. We also believe it would be worthwhile to take a single kernel, slide it across the entire field of view, and compute the correlation at each position (2D correlation map). This approach could be useful, when identifying HXR footpoints. Of course, we can't bypass the need for PIXON algorithm.

3. We overlaid the PFSS field lines on the AIA data for 13:30 UT, whereas the paper does so for 13:15 UT. We believe that no significant non-potential restructuring had occurred in the intervening time, and that the essential topology illustrated in the paper remains preserved.

4. We think it's a good idea include additional radio wavelengths in our wavelet analysis (not just use 2.5 MHz). This may be a sort of validation: if most frequencies give the similar period (within error bars), we can strengthen our case that there's a coherent flare-driven oscillation. We may also find indications of a transition in the emission region.